Journal Homepage: -www.journalijar.com
INTERNATIONAL JOURNAL OF ADVANCED RESEARCH (IJAR)
Article DOI:10.21474/IJAR01/9518
DOI URL: http://dx.doi.org/10.21474/IJAR01/9518

RESEARCH ARTICLE

DETERMINATION OF THE ELECTRICAL PARAMETERS OF A SOLAR CELL BASED ON CIGS UNDER POLYCHROMATIC ILLUMINATION, FROM THE BODE AND NYQUIST DIAGRAMS.

Diallo Demba, Ehemba Alain Kassine, WadeIbrahima And DiengMoustapha.

Manuscript Info

Manuscript History
Received: 06 June 2019
Final Accepted: 08 July 2019
Published: August 2019

Abstract

Nowadays, thin-film solar cells are increasingly used mainly because of their low cost. In recent decades, the performance of these cells has improved significantly. In this work, we simulated a CIGS-based solar cell using new software (SCAPS) to analyze certain parameters. In particular, properties (capacity, capacity derivative, mid-height strip width, parallel resistance and others...) play a crucial role in cell performance, and in order to optimize it. We studied under polychromatic illumination (from 400 nm to 900 nm) their influence on the quantities of the solar cell. In order to highlight the importance of depositing an absorbent layer of the CIGS type on solar cells. The recorded energy efficiency increased from 32.85% to a wavelength of 900 with a form factor FF=80.11% and a form factor FF=81.42% at a wavelength of 600 nm for an efficiency of 23.24% nm. And at this wavelength of 600 nm, we also have a parallel resistance of 2846.9 ohm /cm2. The results obtained are in very good agreement with the published experimental results.

Copy Right, IJAR, 2019,. All rights reserved.

Introduction:-

Numerical electrical and optical simulations of thin-film solar cells are becoming common practice. State of the art polychristalline thin film solar cells, (CIGS) and cadmium telluride (CdTe), and the advanced structures under study, however, never be more complicated [1].

Software tools for digital simulation of solar cells must keep pace with these developments. The SCAPS 3.3.00 electrical program (Solar Cell Capacitance Simulator) is a development of the **University of Gent**, and is available to the photovoltaic research community [2]. In recent years until very recently, its possibilities have been increased as will be illustrated below: (i) Evaluation of the strip space and any other semiconductor properties [3]; this has become a main device in modern CIGS cell structures [4]. (ii) Defects with multiple trade states[5]; amphoteric states not only in amorphous silicon are well known, but also several important defects in CIGS are versatile. (iii) Our knowledge of defects that can change their fitromper state of guration (donor or acceptor) in a metastable manner is quite well established to date [6- 7]; SCAPS can now simulate the effects of these sophisticated properties of materials with measured cell characteristics [8]. (iv) Several mechanisms can be simulated in this software; such as the defect interlayer layers that are essential for describing bifacial cells and tandem and multi-junction cells.

Corresponding Author:-Diallo Demba.

Improving the performance of solar cells requires quality control during the various manufacturing phases. Since the quality of a solar cell is closely linked to its electronic and electrical parameters, different techniques for characterizing these parameters have been developed under different regimes in order to control them during the manufacture of the cell [9].

The purpose of this article is to illustrate the behaviour of the CIGS-based solar cell under polychromatic illumination and at the end to determine some electrical parameters.

Some parameters will be determined from certain methods such as the Nyquist representation (R_S serial resistance and parallel resistance R_p) and the BODE representation (equivalent capacity). From these diagrams, we propose an equivalent electric model of the photopile.

PRESENTATION OF THE STRUCTURE:-

The adapted structure is essentially composed of an n-p cell based on Cu(In, Ga)Se_2 on which is deposited an n-type CdS layer. A diagram of the structure is shown in Figure 1 and Table 1 shows the physical parameters used in the simulation. For fixed parameters such as transmitter, base and window layer ZnO, these values were chosen based on the model of some laboratory structures.

However, to ensure a good metallic contact on this layer, two different options have been developed. One is to open a window in the ZnO layer and the metal contact is made directly on the CIGS.

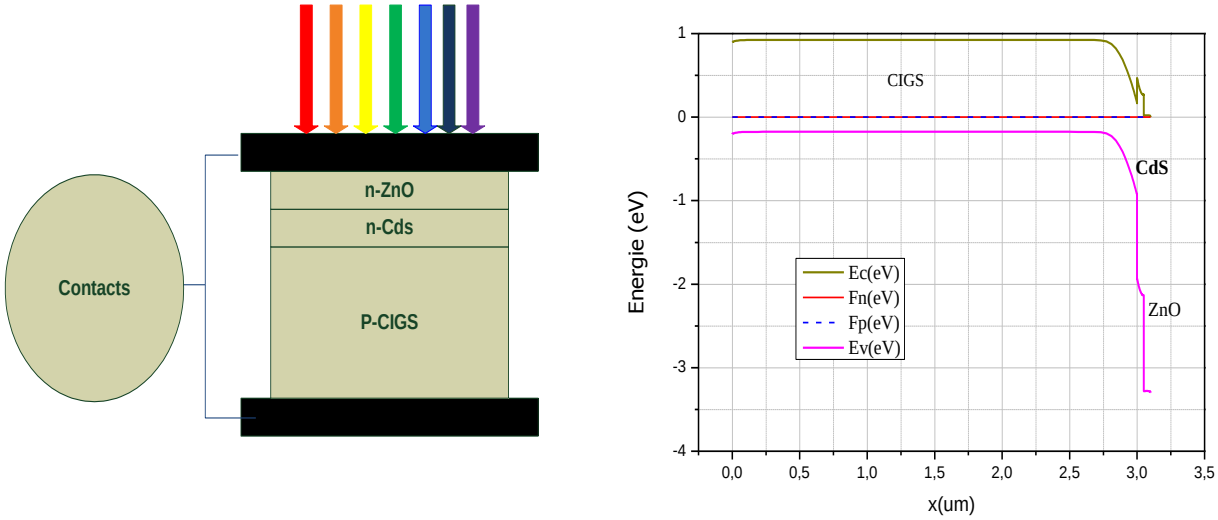

Figure 1:-The cell structure and the proposed Band Diagram of the 1D model used for the simulation.

Table 1:-Physical parameters used in the simulation

	ZnO	CdS	CIGS
Thickness (µm)	0.05	0.05	3
Dielectric constant	9	10	13,6
Electron mobility (cm^2/V.s)	10^2	10^2	10^2
Hole mobility (cm^2/V.s)	$2,5.10^1$	$2,5.10^1$	$2,5.10^1$
Carrier density (cm^{-3})	10^{18}	10^{17}	2.10^{16}
Gap band (eV)	3,3	2,4	1,1
N_c (cm^{-3})	$2,2.10^{18}$	$2,2.10^{18}$	$2,2.10^{18}$
N_v (cm^{-3})	$1,8.10^{19}$	$1,8.10^{19}$	$1,8.10^{19}$
Electronic affinity (eV)	4,45	4,2	4,5

It should be noted that the structure was studied under polychromatic spectrum irradiation (300nm- 900nm), with a power P=100mW/cm^2, and at room temperature T=300°K.

Result and discussion:-

Simulations of the capacity were calculated by performing a small signal analysis at the point operating conditions (naturally with the voltage (*C* - V) and frequency (*C* - f) get changed). The cell structure is then analyzed as if it were a parallel connection of the capacity of a dependent frequency.

The curves shown in this article were traced from OriginPro 2015 software after extracting the data from SCAPS software.

C-V and C-f curves :

Figure 1 shows the variation of the capacitive parameter C as a function of the applied voltage and the variation of the applied light intensity.

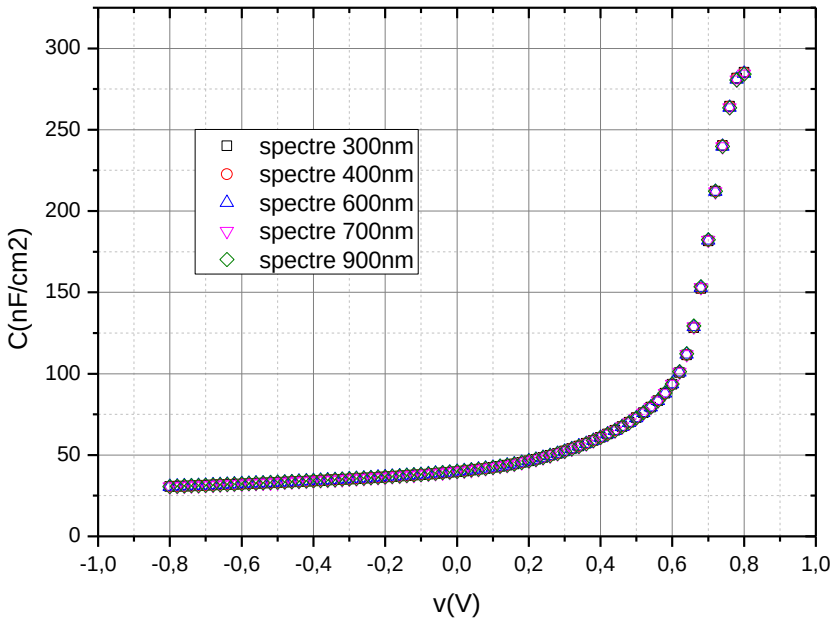

Figure 2:-Simulation curve of the Capacity as a function of voltage for different light intensities.

The value of C changes from 25 to 287.5 nF/cm2. The theoretical curve for diffusion capacity (C≈Cn) is suitable for data taken under dark conditions under dark conditions using Eq. (1):

$$C_n = \frac{aq^2 Ln_0}{k_B T_c} e^{aqV/k_B T} \quad \textbf{(1)}$$

At moderate and high for the room polarization state, increases in diffusion capacity exponentially $C=C_0\, e^{aqV/k_B T}$ due to the profession of electronic DOS by excessive minority charge carriers. The observed variation in scattering capacity with applied polarization indicates the electronic state distribution in the band space and the displacement of the Fermi level. At a higher state of illumination, the introduction of excessive additional holes (Δp) causes an insignificant change in majority holders (p_0).

However, a small change in majority charge carrier causes the Fermi hole that the level at the offset keeps down by $\Delta E_{Fn} = k_B T \ln p_0 /(\Delta p + p_0)$ which is insignificant with respect to the offset of the electron Fermi level. Since the electron carrier density in equilibrium is negligible, the Fermi E_{Fn} level electron changes significantly when excessive carriers are produced at a higher level of illumination and this results in an exponential increase in the diffusion capacity Cu.

We see that capacity increases with tension. We note that also, the variation of the illuminat ion spectrum has almost no influence on the variation. Because in Figure 2, we have almost an overlap of the C-V curves due to the variation of the spectra.

The capacity versus frequency curve was also plotted in Figure 3, where the capacity varies with the variation of the spectra and remains constant with the evolution of the frequency.

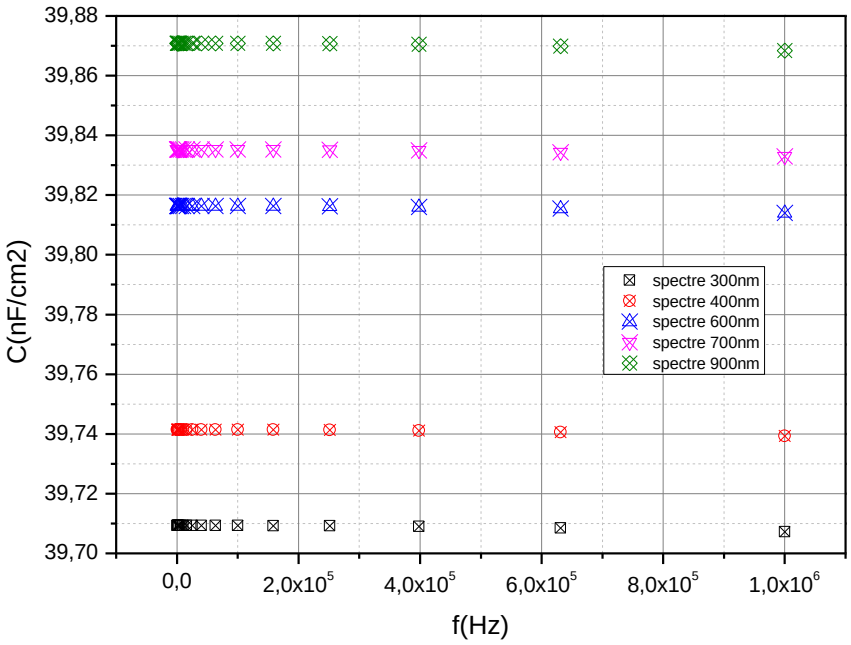

Figure 3:-Simulation curve of the Capacity as a function of frequency for different light intensities.

The main phenomena leading to a capacity transition in CIGS-based solar cells are based on carrier relaxation and defect density.

Determination of the bandwidth at half height [FWHM] from the graph of the capacity derivative as a function of frequency :

There are different processes that can report a step in capacity as a function of frequency. The characteristic frequency capacitance derivative has a specific dependence on the frequency and wavelengths of the spectra as can be seen from (Figure 4)

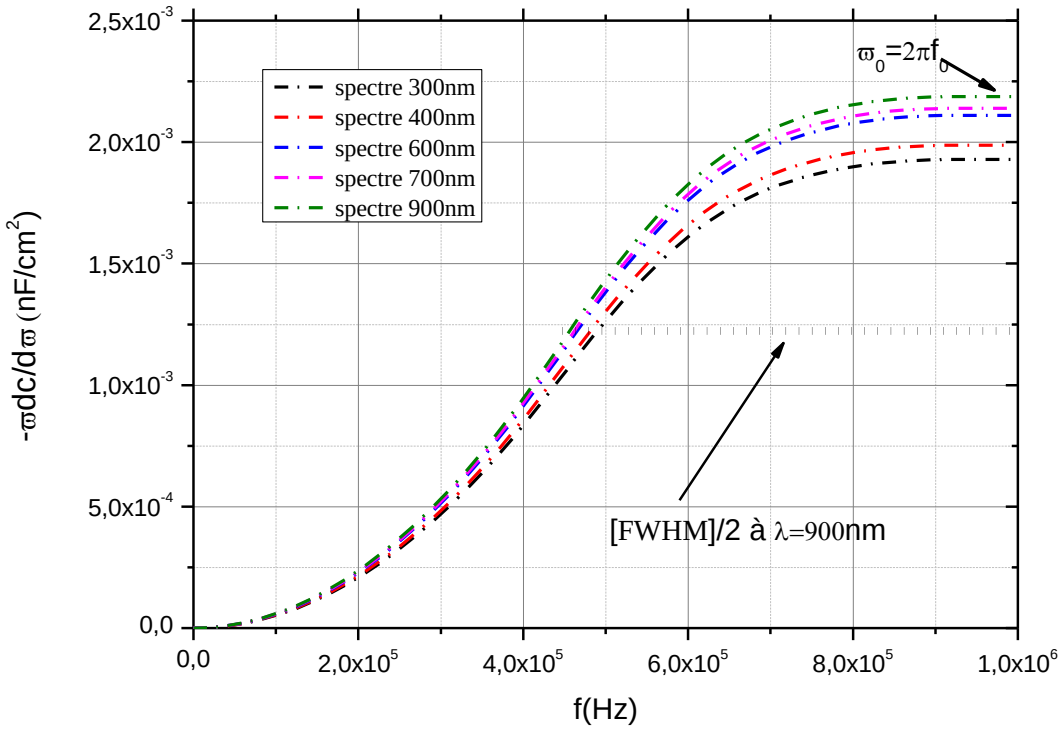

Figure 4:-the frequency curve as a function of the capacity derivative. The bandwidth at half height [*FWHM*].

$$-\omega \frac{\partial C}{\partial \omega}\Big|_{\omega=\omega_0} = \frac{\varepsilon_0 \varepsilon}{2}\left(\frac{1}{w} - \frac{1}{t}\right) \quad (2)$$

$-\omega \frac{\partial C}{\partial \omega}\Big|_{\omega=\omega_0}$ = 2,20.10^{-3} pour λ=900nm

$-\omega \frac{\partial C}{\partial \omega}\Big|_{\omega=\omega_0}$ = 2,15.10^{-3} pour λ=700nm

$-\omega \frac{\partial C}{\partial \omega}\Big|_{\omega=\omega_0}$ = 2,10.10^{-3} pour λ=600nm

$-\omega \frac{\partial C}{\partial \omega}\Big|_{\omega=\omega_0}$ = 2.10^{-3} pour λ=400nm

$-\omega \frac{\partial C}{\partial \omega}\Big|_{\omega=\omega_0}$ = 1,95.10^{-3} pour λ=300nm

The **bandwidth** is thefrequency range of a vibration source. We can also talk about spectrum width. It corresponds to the spectral congestion, i.e. the interval between the low and high frequencies used by the vibration source.
$[FWHM]_{\lambda=300nm}$ = 2×2626 pixels

$[FWHM]_{\lambda=400nm}$ = 2×2668 pixels

$[FWHM]_{\lambda=600nm}$ = 2×2559 pixels

$[FWHM]_{\lambda=700nm}$ = 2×2559 pixels

$[FWHM]_{\lambda=900nm}$ = 2×2559 pixels

A coherent source will have a very low bandwidth, up to monochromatic. This is proven by our simulation where the small bandwidth value is obtained from λ=600nm with a CIGS-based solar cell.

NYQUIST diagram

The NYQUIST diagram consists of representing the imaginary part as a function of the real part of the impedance (Z) of the solar cell.

Measurements were made on the polycrystalline CIGS solar cell under different illumination downstream of the conditions and the impedance spectra are plotted (figure 5) in the complex plane (Zim, Zre), also known as the Nyquist or Cole-school curve [10-11].

To determine the resistances $\mathbf{R_s}$and $\mathbf{R_p}$, we have drawn a representation of Nyquist which is a half circle of center:

$$\begin{pmatrix} \mathbf{Rp + Rs} \\ \mathbf{0} \end{pmatrix}$$

And radius :$\left(\frac{\mathbf{Rp}}{\mathbf{2}}\right)$

Table 2:-Parallel resistance values as a function of wavelength

$\boldsymbol{\lambda(nm)}$	**Rp(ohm/cm^2)**
300	313,11
400	262,04
600	2846,9
700	1371,66
900	511,57

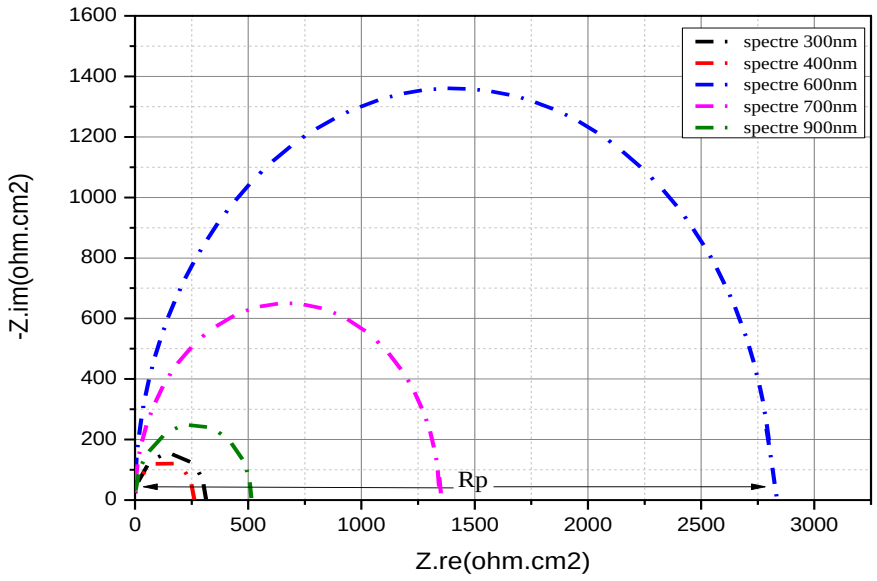

Figure 5:-The impedance spectrum of the polycrystalline CIGS solar cell for different wavelengths.

BODE diagram: dynamic impedance phase

The BODE diagram of the dynamic impedance phase gives the evolution of the phase as a function of the decimal logarithm of the exciter frequency. The Bode diagram provides information on the frequency behaviour of a system. The BODE diagram of the impedance phase of the photopile is given in the figure 6,

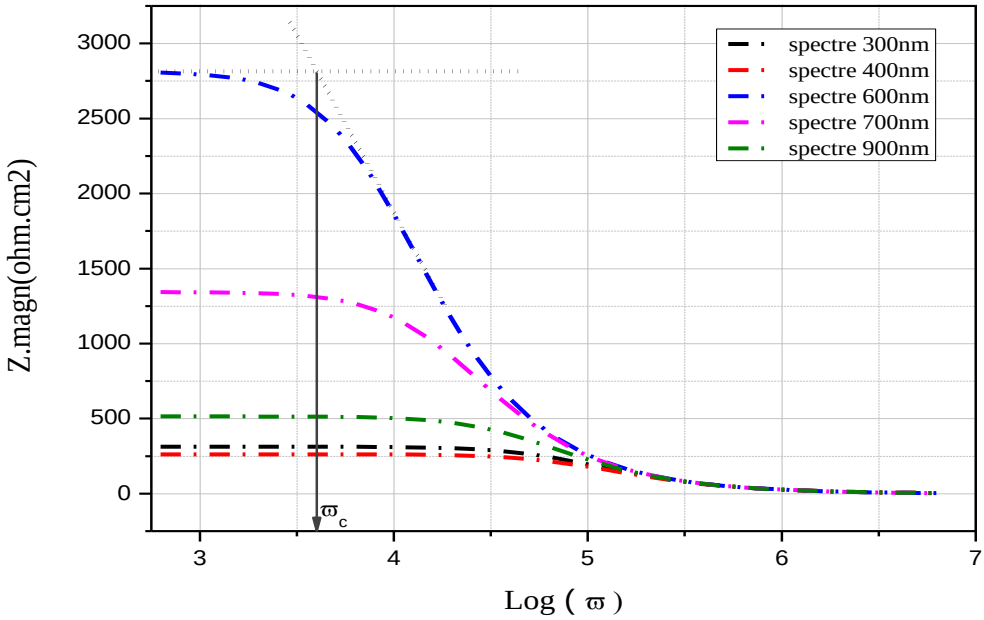

Figure 6:-Impedance modulus as a function of the logarithm of frequency (ω) for polychromatic illumination

The cut-off frequency ω_c :

For angular frequencies within the range $0<\omega<\omega_c$ the dynamic impedance module of the solar cell is frequency independent. And for pulse values such as $\omega>\omega_c$ the impedance modulus decreases with pulse. Thus, the intersection of the extensions of each of the two linear parts of the curve (Figure 6) makes it possible to obtain the angular cut-off pulsation ωc [9].

Table 3:-Cut-off frequency values as a function of wavelength

λ (nm)	**Switching pulse ω_c(rad/s)**
300	$4,1.10^4$
400	$5,34.10^4$
600	4.10^3
700	$9,83.10^3$
900	$2,63.10^4$

The lowest cut-off frequency was obtained at λ =600 nm. This point is determined by the fact that a defect can only contribute to the capacity if the angular frequency is sufficiently low.

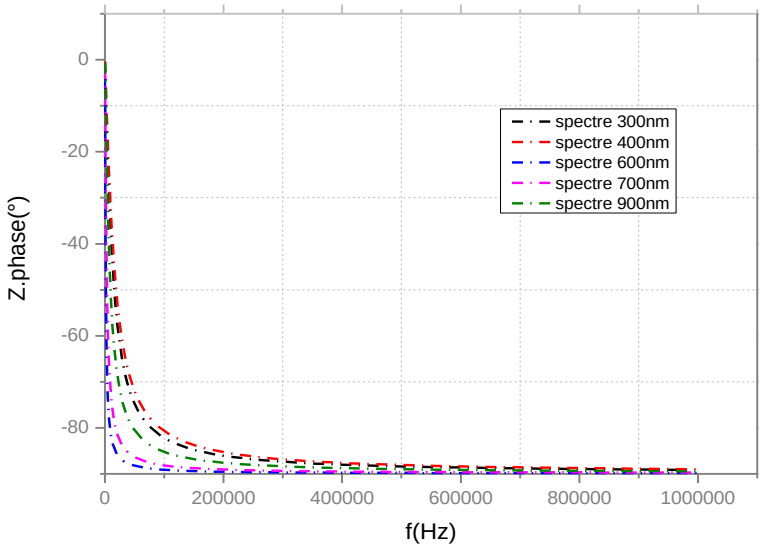

Figure 7:-Impedance phase variation as a function of frequency under different spectra

The appearance of the curves in the figure shows us that:
The impedance phase is negative for wavelengths between 300nm and 900nm. This confirms the presence of a capacitor in the equivalent electrical model of the solar cell.

Knowing the values of the cut-off pulse and the capacity at the (figure) level, we can deduce those of the Shunt Resistance from the following relationship [8]:

$$R_p . C = \frac{2\pi}{\omega_c}$$

Table 4:-Capacity values by wavelength

$\lambda(nm)$	$R_p(\Omega/cm^2)$	ω_c(rad/s)	$C\ (nF/cm^2)$
300	313,11	$4{,}1.10^4$	0,0489
400	262,04	$5{,}34.10^4$	0,0449
600	2846,9	4.10^3	0,0551
700	1371,66	$9{,}83.10^3$	0,0465
900	511,57	$2{,}63.10^4$	0,0467

Thus from the previous remarks we propose the following equivalent electric model:

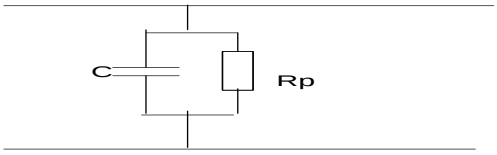

Table 5:-solar cell parameters deduced from calculated IV-curve:

spectre	300 nm	400 nm	600 nm	700 nm	900 nm
Voc	0.570056 Volt	0.603137 Volt	0.621712 Vol	0.625607 Volt	0.631300 Volt
Jsc	8.65 mA/cm2	25.4 mA/cm2	45.91 mA/cm2	53.05 mA/cm2	64.96 mA/cm2
FF	68.4974 %	76.3858 %	81.4238 %	81.0332 %	80.1135 %
eta	3.3810 %	11.7018 %	23.2452 %	26.8956 %	32.8567 %
V_MPP	0.486973 Volt	0.519434 Volt	0.536426 Volt	0.539668 Volt	0.544121 Volt
J_MPP	6.94 mA/cm2	22.53 mA/cm2	43.33 mA/cm2	49.84 mA/cm2	60.38 mA/cm2

With (V_MPP, J_MPP), the coordinates of P_MPP, i. e. the operating point.
The form factor FF is defined as the ratio of the power to the MPP (at the operating point) of the product of the short circuit current and the open circuit voltage: $FF = P_{MPP}/(J_{sc}. V_{oc})$.

Conclusion:-

Cu(In, Ga)$Se_2$is an absorber developed on the back contact layer. It is a layer that has a bandwidth gap between 1.04 eV ($CuInSe_2$) and 2.42 eV for ($CuGaS_2$). The strip space of the alloy can be changed within these margins. Its high absorption coefficient (α > 105 centimetres $^{-1}$ for λ < 600 nm, makes this material very useful as an absorption material. According to our simulation, the largest electrical parameters were obtained for $\lambda=600nm$. This is the case with the Parallel Resistance and the form factor.

Référence:-

1. Advanced electrical simulation of thin film solar cellsMarc Burgelman , Koen Decock, Samira Khelifi, Aimi AbassUniversity of Gent, Electronics and Information Systems (ELIS), Pietersnieuwstraat 41, B-9000 Gent, BelgiumM. Burgelman, P. Nollet, S. Degrave, Thin Solid Films 361 (2000) 527.
2. M. Burgelman, J. Marlein, in: 23rd European Photovoltaic Solar Energy Conference,WIP, Valencia (E), 2008, p. 2151.
3. A. Chirilã, S. Buecheler, F. Pianezzi, P. Bloesch, C. Gretener, A.R. Uhl, C. Fella, L.
4. Kranz, J. Perrenoud, S. Seyrling, R. Verma, S. Nishiwaki, Y.E. Romanyuk, G.
5. Bilger, A.N. Tiwari, Nat. Mater. 10 (2011) 857.
6. K. Decock, S. Khelifi, M. Burgelman, Thin Solid Films 519 (21) (2011) 7481.
7. S. Lany, A. Zunger, Phys. Rev. B 72 (3) (2005) 035215.
8. P. Zabierowski, C. Platzer-Björkman, in: 22nd European Photovoltaic Solar EnergyConference, WIP, München, Milan, I, 2007, p. 2395.
9. K. Decock, P. Zabierowski, M. Burgelman, J. Appl. Phys. 111 (2012) 043703.
10. m. ndiaye , z. nouhou bako, i. zerbo, a. dieng, f. i. barro, g. sissokodetermination des parametres electriques d'une photopile sous eclairementmonochromatique en modulation de frequence, a partir des diagrammes debode et de nyquist
11. S. Kumar, P.K. Singh, G.S. Chilana, S.R. Dhariwal, Generation and recombina- tion life time measure mentin silicon wafers using impedance spectroscopy, Semicond. Sci.Technol.24(2009)095001–095008.
12. K. Pandey, P. Yadav, I.Mukho padhyay, Elucidating different mass flow direction induced polyaniline–ionic liquid interface properties: insight gained from DCvoltammetryandimpedancespectroscopy, J.Phys.Chem.B.118 (2014)3235–3242.